# Two-center effects in one-photon single ionization of $H_2^+$, $H_2$, and $Li_2^+$ with circularly polarized light

J. Fernández,[1,*] F. L. Yip,[2] T. N. Rescigno,[2] C. W. McCurdy,[2,3] and F. Martín[1]
[1]*Departamento de Química, C-9, Universidad Autónoma de Madrid, 28049 Madrid, Spain*
[2]*Lawrence Berkeley National Laboratory, Chemical Sciences, Berkeley, California 94720, USA*
[3]*Departments of Applied Science and Chemistry, University of California, Davis, California 95616, USA*
(Received 12 November 2008; revised manuscript received 26 February 2009; published 9 April 2009)

We present a theoretical study of one-photon single ionization of $H_2^+$, $H_2$, and $Li_2^+$ with circularly polarized light of a few hundred eV (a few tens of eV for $Li_2^+$). At these photon energies, two-center interference effects due to confinement and double-slit diffraction are expected. The results show that, in general, the calculated angular distributions for circularly polarized light are very similar to those obtained by incoherently averaging the angular distributions for parallel and perpendicular linearly polarized light. Thus, at the lower photon energies, the multiple lobes observed in the angular distributions for circularly polarized light (which are absent for linearly polarized light) have little to do with confinement and/or double-slit diffraction. At the higher photon energies, such effects do exist, but they are partly hidden and are much more difficult to analyze than for linearly polarized light. The simple diffraction interpretation is even less applicable for $H_2$ and $Li_2^+$ because confinement and double-slit diffraction appear at electron energies too low to ignore electron correlation and the details of the molecular potential.

DOI: 10.1103/PhysRevA.79.043409 PACS number(s): 33.80.Eh

## I. INTRODUCTION

Recent experimental and theoretical work [1–18] has shown that interferences similar to those observed by Young in his famous double-slit experiment can be observed in molecular ionization when the wavelength $\lambda_e$ of the ejected electron is comparable to or smaller than the size of the molecule. For the $H_2$ molecule, such interferences are expected when $\lambda_e \leq 0.74$ Å (1.4 a.u.), where the latter number is the $H_2$ equilibrium internuclear distance $R_e$. Electron wavelengths this short can be achieved by ionizing the molecule with photons of a few hundred eV, which are available in modern synchrotron-radiation facilities.

The prediction of double-slit interferences in molecular photoionization was made by Cohen and Fano [19], who explained the presence of oscillations in the integral photoionization cross section as a function of photon energy (see also [6,9]). These oscillations, however, are superimposed on a rapidly decreasing monotonic background, which makes the observation extremely difficult [1,3]. Much clearer evidence of double-slit interferences can be obtained by analyzing the electron angular distributions arising from fixed-in-space molecules. This idea, first proposed by Kaplan and Markin [20], has been followed in recent theoretical work [14,21] to investigate the origin of the interferences when linearly polarized light is used. In the latter work, it was shown that, for $H_2$ molecules oriented parallel to the polarization direction, the angular distribution exhibits "partial-wave confinement" when $k_e R \sim \ell\pi$ (where $k_e = 2\pi/\lambda_e$, $R$ is the internuclear distance, and $\ell$ is the asymptotic angular momentum of the electron in the continuum), while for molecules oriented perpendicularly, it exhibits typical interference patterns with maxima given by the well-known Young's formula $R \sin\theta_e \sim n\lambda_e$ (where $\theta_e$ is the electron emission angle referred to the polarization direction). Similar conclusions have also been found for $H_2^+$ photoionization. It was also shown that, for $H_2$, the angular distributions strongly depend on the energy sharing between electrons and nuclei and that the vibrational distribution of the residual ion does not follow the usual Franck-Condon distribution in the parallel geometry. Hence there is a need to properly include the nuclear motion in the $H_2$ calculations.

Experimentally, the idea of studying interference effects by looking at the electron angular distributions has been recently realized in kinematically complete cold target recoil ion momentum spectroscopy (COLTRIMS) experiments [13] in which $H_2$ is doubly ionized by absorption of circularly polarized synchrotron radiation of about 200 eV. From the experimental point of view, the study of double photoionization is ideal because this process leads to two protons that can be detected in coincidence without any ambiguity. However, the fact that not only one but the two electrons are ejected may obscure the analysis. Indeed, correlation is the essential property that allows both electrons to be ejected simultaneously. In the absence of correlation, the probability of double ionization by absorption of a single photon is exactly zero if screening is also neglected in the neutral molecule. However the correlated interaction of the two electrons can significantly distort the interference patterns that are expected when a single electron is diffracted by two nuclei. For this reason, in the experiments of Ref. [13], it was proposed that the usual double-slit interferences should only be apparent for extreme unequal energy sharing between the electrons (i.e., one electron is much faster than the other one thus minimizing the relative importance of correlation) and for electron angular distributions integrated over the emission direction of the slow electron (doubly differential cross sections).

This interpretation has been confirmed by theoretical calculations that explicitly include electron correlation [18], al-

*Present address: Department of Physics and Astronomy, Lundbeck Foundation Theoretical Center for Quantum System Research, University of Aarhus, 8000 Aarhus C, Denmark.

 

though they show that double-slit interferences appear in fact at higher photon energies than those used in the experiment. The calculations of [18] also show that the use of circularly polarized light introduces an additional complication in the analysis of the experimental data since the angular distributions result from the interference of $\Sigma_u^+$ and $\Pi_u$ amplitudes which, if analyzed separately as in experiments with linearly polarized light, allow one to unambiguously detect double-slit interferences or confinement effects as those described above.

In order to analyze the consequences of using circularly polarized light without the additional complication of having two electrons in the continuum, we have investigated one-photon single ionization of $H_2^+$, $H_2$, and $Li_2^+$ with circularly polarized light. In $H_2^+$ photoionization, electron correlation is totally absent. In single ionization of $H_2$, correlation is expected to play a much less important role than in double ionization except when doubly excited states are populated [22], which is not the case at the large photon energies considered in this work. The same is expected in single ionization of $Li_2^+$, since we will consider emission of the only valence electron of the molecule (the role of the inner electrons is primarily to screen the potential seen by the valence electron). In addition, the choice of these three systems will also allow us to investigate the variation in interference effects with the distance between the two diffractive centers (1.4 a.u. for $H_2$, 2.0 a.u. for $H_2^+$, and 5.9 a.u. for $Li_2^+$) and to analyze the role of electron correlation and screening by comparing $H_2$ and $Li_2^+$ results with those obtained from an $H_2^+$ molecular ion artificially compressed and stretched to internuclear distances of 1.4 and 5.9 a.u., respectively. The present theoretical study is relevant in view of experiments in progress at the SOLEIL synchrotron-radiation facility on one-photon single ionization of $H_2$ by using circularly polarized light. Angular distributions obtained in these experiments at photon energies of about 30 eV (see also [23,24]) indicate that the additional $\Sigma_u^+ - \Pi_u$ coherence induced by the circular polarization may indeed hide physical effects that are clearly visible with linearly polarized light. If this is the case for single ionization, then the use of circularly polarized light might not be the optimum choice to analyze double-slit interferences in double ionization.

This paper is organized as follows. In Sec. II, the theoretical methods, which have been successfully used in previously published work [14,17,22,25], will be briefly summarized. Then, in Sec. III, the calculated angular distribution (differential in the energy and direction of the ejected electron and the energy and orientation of the residual molecular ion) will be presented. Also the validity of existing models [13,26] for circularly polarized light will be discussed. Conclusions and future perspectives will be presented in Sec. IV. Atomic units are used throughout unless otherwise stated.

## II. THEORETICAL METHODS

The theoretical methods have been described in detail in previous work [17,21,22]. Here we only summarize the basic equations. The fully differential photoionization cross section, i.e., differential in both the energy and direction of the ejected electron and the energy and orientation of the residual molecular ion, is given by Dill's formula [27],

$$\frac{d\sigma_\alpha^{\mu_0}(\omega)}{d\Omega_n d\Omega_e d\varepsilon} = \frac{4\pi^2\omega}{c} \sum_{\mu_a,\mu_b} \sum_{\ell_a,m_a} \sum_{\ell_b,m_b} i^{(\ell_a-\ell_b)} e^{i[\hat{\sigma}_{\ell_a}(\varepsilon)-\hat{\sigma}_{\ell_b}(\varepsilon)]} (-1)^{m_b+\mu_a-\mu_0} T^*_{\alpha\ell_a m_a\mu_a}(\varepsilon) T_{\alpha\ell_b m_b\mu_b}(\varepsilon)$$
$$\times \sum_{L_e} \left[\frac{(2\ell_a+1)(2\ell_b+1)}{(2L_e+1)}\right]^{1/2} C(\ell_a,\ell_b,L_e;-m_a,m_b,M_e) C(\ell_a,\ell_b,L_e;0,0,0) Y^{M_e*}_{L_e}(\theta_e,\phi_e)$$
$$\times \sum_{L_\gamma} \left[\frac{1}{(2L_\gamma+1)}\right]^{1/2} C(1,1,L_\gamma;-\mu_a,\mu_b,M_\gamma) C(1,1,L_\gamma;-\mu_0,\mu_0,0) Y^{M}_{L_\gamma\gamma}(\theta_n,\phi_n), \quad (1)$$

with $\mu_{a,b}=0, \pm 1$, $M_\gamma=-\mu_a+\mu_b$, $M_e=-m_a+m_b$, $\ell_a+\ell_b \geq L_e \geq |\ell_a-\ell_b|$, and $2 \geq L_\gamma \geq 0$. In this equation, $\mu_0=0$ for linearly polarized light and $\mu_0=\pm 1$ for circularly polarized light, $\alpha$ denotes the electronic state of the residual molecular ion, $\hbar\omega$ is the photon energy, $\varepsilon$ is the photoelectron energy, $\Omega_e=(\theta_e,\phi_e)$ is the photoelectron emission direction in the molecular frame ($\theta_e$ and $\phi_e$ are the polar angles), $\Omega_n=(\theta_n,\phi_n)$ is the polarization direction with respect to the molecular axis $z$, $c$ is the speed of light, $C(j_1,j_2,j;m_1,m_2,m)$ denotes a Clebsch-Gordan coefficient, $Y_L^M$ is a spherical harmonic, $\hat{\sigma}_\ell(\varepsilon)$ is the Coulomb phase shift, and $T_{\alpha\ell m\mu}(\varepsilon)$ is the transition matrix element evaluated in the framework of the dipole approximation,

$$T_{\alpha\ell m\mu}(\varepsilon) = \int dR \langle \Psi_{g\nu}(\mathbf{r},R) | \mathbf{e}_\mu \cdot \mathbf{D} | \Psi^+_{\alpha\nu_\alpha\ell m\varepsilon}(\mathbf{r},R) \rangle, \quad (2)$$

where $\Psi_{g\nu}$ is the ground molecular state of energy $W_{g\nu}$, $\Psi^+_{\alpha\nu_\alpha\ell m\varepsilon}$ is the final molecular state of energy $W_{\nu_\alpha}+\varepsilon$ representing a molecular ion in the $\nu_\alpha$ vibronic state (either dissociative or nondissociative) and an ionized electron of energy $\varepsilon$ and angular momentum $\ell m$, $\mathbf{r}$ represents the electronic coordinates, $R$ is the internuclear distance, $\mathbf{e}_\mu$ is the photon polarization vector, and $\mathbf{D}$ is either $\Sigma_i \mathbf{r}_i$ (length gauge) or $(\hbar\omega)^{-1}\Sigma_i \nabla_i$ (velocity gauge). Energy conservation implies that $W_{g\nu}+\hbar\omega=W_{\nu_\alpha}+\varepsilon$.

To evaluate the $H_2^+$ and $H_2$ wave functions, we have followed the procedures of Refs. [21,22,25]. Neglecting rotational effects, the wave functions $\Psi_{g\nu}$ and $\Psi^+_{\alpha v_\alpha \ell m\varepsilon}$ are obtained in the adiabatic [Born-Oppenheimer (BO)] approximation

$$\Psi_{nv_n}(\mathbf{r},R) = R^{-1}\chi_{v_n}(R)\psi_n(\mathbf{r},R), \tag{3}$$

where $\psi_n$ and $\chi_{v_n}$ are the usual electronic and nuclear BO wave functions [22,25]. For each value of $R$, the electronic continuum states must satisfy the usual outgoing boundary conditions of electron-molecule scattering.

In the case of $H_2^+$ photoionization, it has been shown [14,21] that angular distributions calculated by ignoring the nuclear motion are practically identical to those obtained by including the nuclear motion when the relative proton kinetic energy is equal to $1/R$. This is because, as a consequence of the repulsive character of the potential-energy curve of the ionized molecular ion, there is an almost perfect mapping of the internuclear distance at which ionization takes place and the relative kinetic energy of the two protons. This is also the case for double photoionization of $H_2$ [28]. One can expect that the reflection approximation will also work in the case of $Li_2^+$ photoionization because the potential that describes the ionized $Li_2^+$ molecule is also repulsive. Thus, to study $Li_2^+$ photoionization, the transition matrix element has been written

$$T_{\alpha\ell m\mu}(\varepsilon) = \langle \Psi_g(\mathbf{r},R_e)|\mathbf{e}_\mu \cdot \mathbf{D}|\Psi^+_{\alpha\ell m\varepsilon}(\mathbf{r},R_e)\rangle, \tag{4}$$

where integration over the internuclear distance is no longer needed and the molecular wave functions only include the electronic part evaluated at $R=R_e$,

$$\Psi_n(\mathbf{r},R_e) = \psi_n(\mathbf{r},R=R_e). \tag{5}$$

For $H_2^+$ and $H_2$, the computational methods used to obtain the wave functions included in the $T_{\alpha\ell m\mu}$ matrix elements have been successfully applied to study a variety of different ionization problems, such as resonant dissociative photoionization [22,25,29–31] and ion impact ionization [32]. More specifically, the vibrational (bound and dissociative) wave functions have been expanded in a basis of 280 B-splines of order $k=8$ contained in a box of 12 a.u. Molecular orbitals are written in terms of a one-center expansion that includes spherical harmonics up to $\ell=16$. For each $\ell$, the corresponding radial part has been expanded in a basis of 310 B-splines of order $k=8$ in a box of radial length of 60 a.u. For $H_2$, the ground state $\Psi_g$ results from a configuration-interaction (CI) calculation in which the $H_2$ Hamiltonian has been diagonalized in a basis of 321 configurations built from products of one-electron $H_2^+$ orbitals and pseudo-orbitals. The calculated energy at the equilibrium internuclear distance is −1.886 502 3 a.u., to be compared with the exact nonrelativistic value −1.888 761 38 a.u. [33]. The final electronic continuum state $\Psi^+_{\alpha v_\alpha \ell m\varepsilon}$ results from a close-coupling calculation that includes all partial waves with $\ell \leq 7$ associated with the four lowest ionization thresholds of $H_2$: $X\,^2\Sigma_g^+(1s\sigma_g)$, $^2\Sigma_g^+(2p\sigma_u)$, $^2\Pi_u(2p\pi_u)$, and $^2\Sigma_g^+(2s\sigma_g)$ (see Ref. [21] for more details).

In the case of $Li_2^+$, the large internuclear separation makes a one-center expansion impractical. Therefore, the electronic wave functions of $Li_2^+$ were evaluated with a hybrid basis as described in [17]. Briefly, the coordinates of the electrons are represented using a mixed basis involving traditional Gaussian basis functions and a finite element discrete variable representation (FEM-DVR) with exterior complex scaling (ECS) [34]. This "hybrid" basis permits the description of the closed-shell core electrons using standard quantum chemistry techniques while allowing for the interaction with the photoelectron to be accounted for in the continuum final state. A basis of 72 primitive and contracted Gaussian basis functions was found to sufficiently span a spherical inner region defined just beyond the location of the nuclei and provide adequate description of the core electrons. The outer DVR region was composed of 17th order DVR in finite elements of length 10 bohr up to the exterior complex scaling turning point located at $r=50.0$ bohr. In the outer region, where the FEM-DVR basis functions are associated with asymptotic partial-wave contributions to the wave function, partial waves up to $\ell=7$ were used to converge the calculated angular distributions. This basis was found to be sufficient for representing the bound and continuum states of $Li_2^+$ over a wide range of molecular internuclear distances and photon energies [17], including those reported here.

## III. RESULTS

In all figures presented below, we will consider right handed linearly polarized light with incidence direction perpendicular to the molecular axis. This special geometry leads to the coherent mixing of the $\Sigma_u^+$ and $\Pi_u$ amplitudes. In other words, if one considers that the incidence direction is along the $y$ axis, the corresponding transition amplitude will involve the dipole operator $x+iz$, which is a superposition of the dipole operators $z$ and $x$ associated with the $\Sigma_u^+$ and $\Pi_u$ amplitudes. The latter amplitudes describe transitions induced by linearly polarized light parallel and perpendicular to the molecular axis. For this reason, to analyze the importance of the $\Sigma_u^+ - \Pi_u$ mixing, we will always compare our results for circularly polarized light with those for linearly polarized light both in the parallel and the perpendicular geometrical arrangements.

The condition to observe confinement effects in the parallel geometry is approximately given by the formula $k_eR = \ell\pi$ [14,21,35], which can also be written in terms of the energy of the ionized electron as

$$\varepsilon = \frac{\ell^2\pi^2}{2R^2}. \tag{6}$$

In the perpendicular case, constructive interferences are expected at emission angles approximately given by Young's formula $\sin\theta_e = n\lambda_e/R$; since $n\lambda_e/R$ must be smaller than one, the energy threshold above which one expects double-slit interferences is approximately given by

$$\varepsilon > 2\pi^2/R^2. \tag{7}$$

Figure 1 shows the calculated electron angular distribution for $H_2^+$ for photon energies of 5.0 and 9.5 a.u. The chosen

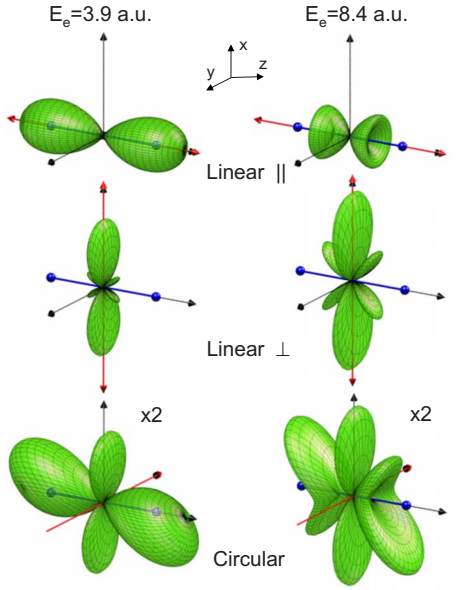


FIG. 1. (Color online) Electron angular distribution in $H_2^+$ photoionization. Upper panels: results obtained with linearly polarized light with $H_2^+$ oriented parallel ($\Sigma_u^+$ symmetry) to the polarization direction. Middle panels: idem with $H_2^+$ oriented perpendicularly ($\Pi_u$ symmetry) to the polarization direction. Lower panels: results obtained with circularly polarized light with incidence direction perpendicular to the $H_2^+$ molecular axis. Angular distributions corresponding to electrons ejected with energies of 3.9 and 8.4 a.u. for photon energies of 5.0 and 9.5 a.u., respectively, are shown by three-dimensional plots in green. In the case of linearly polarized light, the polarization direction is indicated by the double arrow (red). In the case of circularly polarized light, the red arrow indicates the incidence direction (pointing towards the negative part of the $y$ axis). The two nuclei are indicated by two small spheres (blue).

electron energies are 3.9 and 8.4 a.u., respectively, which are close to the maxima of the corresponding proton kinetic energy distributions (i.e., they correspond to the electron energies that would be obtained in a vertical transition, see [14,21]). By using the simple formulae (6) and (7) with $R=R_e$, one concludes that, at the larger electron energy, both confinement (for $\ell=3$) and double-slit effects are expected in the angular distributions associated with parallel and perpendicular linearly polarized light, respectively, while none (or almost none) of these effects should be expected at the lower electron energy. This is clearly illustrated in Ref. [21] and in Fig. 1 for linearly polarized light. At the lower electron energy, the angular distributions exhibit two lobes that follow the direction of the light electric field. In the perpendicular case, the presence of two small additional lobes suggests the existence of double-slit interferences even below the threshold. In contrast, at the higher electron energy, the angular distribution does not exhibit this typical two-lobed pattern: in the parallel case it presents a dip along the polarization direction (indicating that the preference of the electron is no longer to follow the polarization direction) while, in the perpendicular case, additional lobes on both sides of the dominant lobe clearly indicate the presence of double-slit interferences.

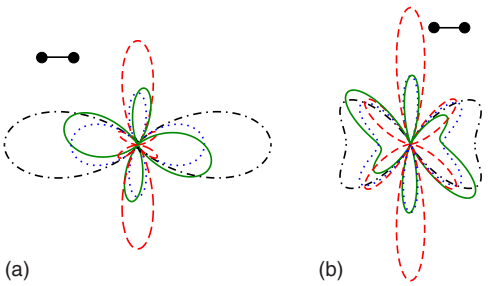


FIG. 2. (Color online) Comparison between $H_2^+$ angular distributions obtained with linearly and circularly polarized light in the plane containing the polarization vector and the molecular axis. (a) Photon energy, 5.0 a.u.; electron energy, 3.9 a.u. (b) Photon energy, 9.5 a.u.; electron energy, 8.4 a.u. Dashed-dotted line: linearly polarized light parallel to the molecular axis; dashed line: linearly polarized light perpendicular to the molecular axis; full line: circularly polarized light with incidence direction perpendicular to the molecular axis; dotted line: arithmetic average of the results for parallel and perpendicular linearly polarized light.

At first sight, the angular distribution obtained with circularly polarized light exhibits a superposition of the dominant effects observed for parallel and perpendicular linearly polarized light. However, the combination of such effects may suggest the existence of double-slit interferences where there are none or, the other way around, obscure them when they are not dominant. The results shown in the left column of Fig. 1 are a clear illustration: the additional lobes seen in the angular distributions for perpendicular linearly polarized light, which are the signature of double-slit effects, are hidden in the results for circularly polarized light. At lower photon energies, the additional lobes seen in Fig. 1 for the perpendicular case are not seen any more, which is a clear indication of the absence of double-slit interference effects. However, the corresponding angular distribution for circularly polarized light still exhibits four prominent lobes that, therefore, cannot be interpreted as due to double-slit interference effects.

Figure 2 shows a direct comparison between the three angular distributions in the plane that contains the molecular axis and the polarization direction ($xz$ plane in Fig. 1). The figure also shows the arithmetic average of the angular distributions associated with the parallel and perpendicular cases. As can be seen, the latter distributions are very similar to those obtained with circularly polarized light except for the slight rotation of the real angular distribution that is due to the rotation of the polarization vector in the same direction. This twist of the angular distribution with respect to the arithmetic average is due to coherence between the $\Sigma_u^+$ and $\Pi_u$ amplitudes. In any case, the coherence is rather small because of the little overlap between the $\Sigma_u^+$ and $\Pi_u$ angular distributions.

The above conclusions remain approximately valid for $H_2$. Figure 3 shows the calculated electron angular distribution for $H_2$ for photon energies of 2.5, 6.0, and 13.0 a.u. The chosen electron energies are 1.9, 5.4, and 12.4 a.u., respectively, which nearly correspond to the maxima of the corresponding vibrational distributions of the remaining $H_2^+$ ion (i.e., they correspond to the electron energies associated with

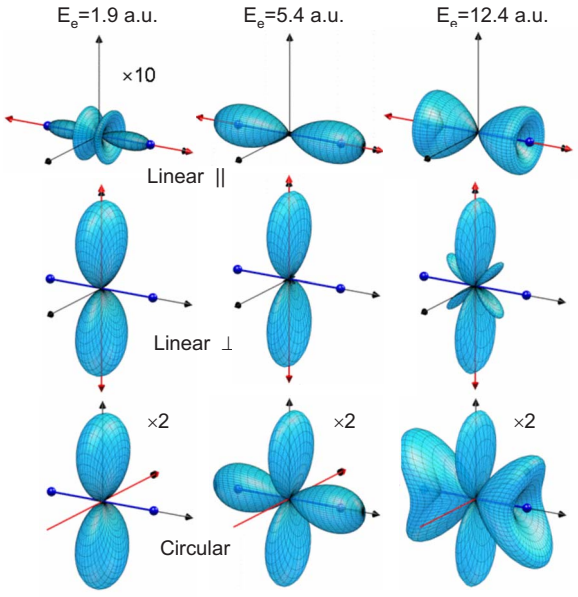


FIG. 3. (Color online) As in Fig. 1, but for $H_2$ photoionization that leaves the residual $H_2^+$ ion in the $v=2$ vibrational state. Three cases are shown: photon energies of 2.5, 6.0, and 13.0 a.u. that correspond to electron energies of 1.9, 5.4, and 12.4 a.u., respectively.

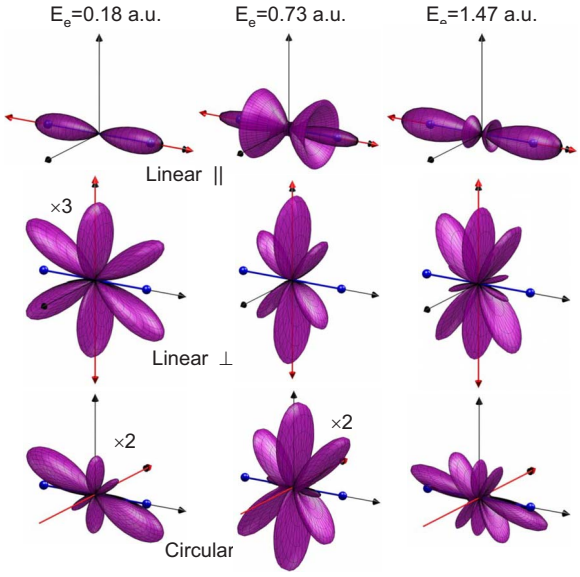


FIG. 4. (Color online) As in Fig. 1 but for $Li_2^+$ photoionization. Three cases are shown: electron energies of 0.18, 0.74, and 1.47 a.u. for photon energies of 0.6, 1.1, and 1.9 a.u., respectively.

in an almost vertical transition that leaves $H_2^+$ in the $v=2$ vibrational state, see [14,21]). According to the simple formulae (6) and (7) discussed above, confinement effects are only expected at the lowest electron energy (1.9 a.u.), while double-slit effects are only expected at the largest electron energy (12.4 a.u.). These expectations are supported by the angular distributions reported in [21] and by those shown in Fig. 3 for linearly polarized light parallel and perpendicular to the molecular axis (the parallel case at 12.4 a.u. seems to suggest the existence of some confinement whose origin has been discussed in detail in Ref. [21]). For circularly polarized light, the angular distributions exhibit again a combination of the main patterns already observed for linearly polarized light. A similar analysis as that shown in Fig. 2 reveals that coherence between the $\Sigma_u^+$ and $\Pi_u$ amplitudes plays again a minor role except for the small twist of the distribution in the direction of rotation of the polarization vector. This is less obvious for an electron energy of 1.9 a.u., because the $\Sigma_u^+$ contribution is much smaller than the $\Pi_u$ one and because this energy is probably too low to assume that coherence between the $\Sigma_u^+$ and $\Pi_u$ amplitudes is negligible.

Finally, we present our results for $Li_2^+$. In principle, one would expect that this system behaves as $H_2^+$. However, the unusually large value of its equilibrium internuclear distance (5.9 a.u.) implies, according to the simple formulae (6) and (7), that confinement and double-slit effects should appear at much lower energies, namely, 0.14 and 0.57 a.u. However, at such low electron energies, the validity of those formulae is uncertain since they are based on the assumption that the ionized electron does not see the details of the molecular potential except at the position of the nuclei. Figure 4 shows the angular distributions obtained at photon energies of 0.6, 1.1, and 1.9 a.u. As mentioned in Sec. II, in this case the calculations have been performed in the framework of the fixed-nuclei approximation. Therefore, the electron energies are simply given by the difference between the photon energy and the vertical ionization potential of $Li_2^+$, 0.18, 0.74, and 1.47 a.u. It can be seen that, for linearly polarized light, the angular distributions do not follow the typical two-lobed pattern observed in $H_2^+$ and $H_2$ at the lower energies. In the perpendicular case, the angular distributions exhibit additional lobes on both sides of the central lobe that follows the polarization direction. The number of these lobes increases with energy, which is consistent with the image of a double slit; however, second-order additional lobes appear at much lower energies than predicted by Eq. (7). In the parallel case, the angular distributions suggest the existence of confinement but the electron energies do not follow Eq. (6). This is probably due to the fact that, for the reasons mentioned above, the quantitative value of these simple formulae is much more limited at low electron energies. In spite of this, the angular distributions obtained with circularly polarized light exhibit a combination of the main patterns observed for linearly polarized light. In this case, the angular distributions exhibit a larger rotation with respect to those obtained from the incoherent sum of the $\Sigma_u^+$ and $\Pi_u$ amplitudes, but all in all the position and shape of the different lobes can be easily inferred from the results for linearly polarized light. In any case, it is clear that interferences between the $\Sigma_u^+$ and $\Pi_u$ amplitudes are more important in $Li_2^+$ than in $H_2^+$ and $H_2$, which is the consequence of the low electron energies that are expected to lead to confinement and double-slit interferences in $Li_2^+$. At higher energies, one would expect that such simple models would work better, but the number of nodes would be so large that the angular distributions would be of little use to investigate these ideas.

In order to analyze the role of electron correlation and screening in $H_2$ and $Li_2^+$, we have compared their angular distributions with those obtained from an $H_2^+$ molecular ion

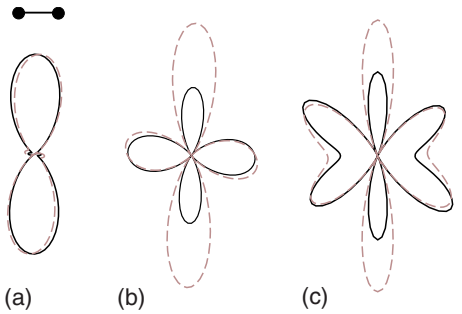


FIG. 5. (Color online) Comparison between the $H_2$ angular distributions obtained with circularly polarized light (full lines) and those obtained from an artificial $H_2^+$ molecule with fixed $R=1.4$ a.u. (dashed lines). The $H_2^+$ distributions have been renormalized to the values at the maximum of the horizontal lobes in the $H_2$ distributions. Electron energies are the same as in Fig. 3.

artificially compressed and stretched to internuclear distances of 1.4 and 5.9 a.u., respectively. The results are presented in Figs. 5 and 6. It can be seen that there are significant differences between the $H_2$ and the $H_2^+$ distributions as well as between the $Li_2^+$ and the $H_2^+$ ones. Although the number of lobes in the $H_2$ and artificial $H_2^+$ distributions is the same, the relative magnitude of these lobes is very different. This implies that electron correlation does play a role in the angular distributions for single ionization even at high energy. The same applies to $Li_2^+$ at the electron energy shown in Fig. 6, but the disagreement with the artificial $H_2^+$ angular distributions becomes even larger at electron energy decreases (not shown). This is because screening of the nuclear charge by core electrons is not complete and, consequently, the potential felt by the ionized electron is significantly different in the two cases (see Ref. [17] for details). As we will see below, this has important consequences when one tries to use one-electron models for quantitative predictions of electron angular distributions.

In the case of $H_2^+$ photoionization by linearly polarized light, the angular distributions approximately follow the formula [26] $(\mathbf{e}_\mu \cdot \mathbf{k}_e)^2 \cos^2(\mathbf{k}_e \cdot \mathbf{R}/2)$. If $\mathbf{e}_\mu$ and $\mathbf{k}_e$ are parallel to the molecular axis, this formula leads to zero when $k_e R = \pi, 3\pi, \ldots$, i.e., no electron emission along the molecular axis in agreement with the image of confinement. As mentioned in previous work [14], a similar formula describes in classical optics the interference produced at long distances by two radiating dipole antennas separated a distance $R$. For $H_2$, the predictive value of the above model is more limited because one cannot rely on the reflection approximation to deduce the value of $R$. However, as shown in [21], the formula still works at the highest photon energies if one uses for $R$ the value of the inner classical turning point $R_{in}$ associated with the $H_2^+$ vibrational levels instead of $R=R_e$. For $Li_2^+$, one would expect a similar validity as for $H_2^+$ since one can rely again on the reflection approximation to unambiguously define $R=R_e$.

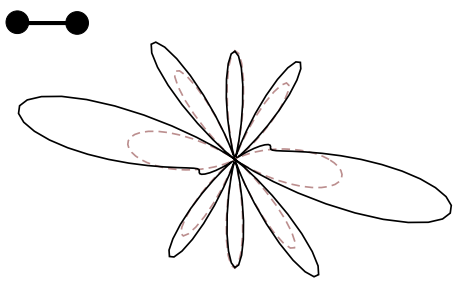

FIG. 6. (Color online) Comparison between the $Li_2^+$ angular distribution obtained with circularly polarized light (full lines) and that obtained from an artificial $H_2^+$ molecule with fixed $R=5.9$ a.u. (dashed lines). The $H_2^+$ distribution has been renormalized to the value at the maximum of the vertical lobes in the $Li_2^+$ distribution. The electron energy is 1.47 a.u., the largest in Fig. 4.

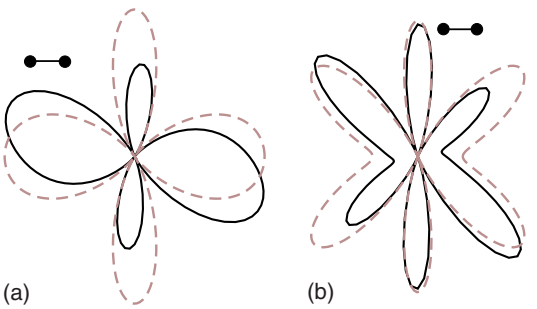


FIG. 7. (Color online) Comparison between the $H_2^+$ angular distributions obtained with circularly polarized light (full line) and those obtained from the model formula $\cos^2(\mathbf{k}_e \cdot \mathbf{R}_e/2)$ (dashed line) at the same photon and electron energies as in Fig. 1.

For circularly polarized light, the model can be easily extended. In this case, the angular distribution should follow the formula $\cos^2(\mathbf{k}_e \cdot \mathbf{R}/2)$ [13], which results from applying the above model amplitudes for parallel and perpendicular linearly polarized light and combining them in the usual way. Figures 7–9 show a comparison of the calculated angular distributions and the model ones for circularly polarized light. It can be seen that the model explains qualitatively the shapes of the distributions but it does not account for either the relative magnitude of the different lobes or the slight rotation of the calculated angular distributions.

The situation is different for the case of $Li_2^+$. The large internuclear distance of $Li_2^+$ results in a more nonspherical interaction potential for the exiting electron than in either $H_2$ or $H_2^+$. Thus, at the lower energies, there are large high angular-momentum contributions, in particular very substan-

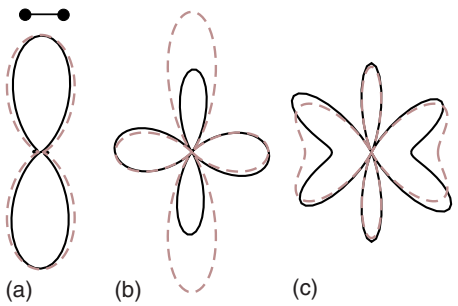


FIG. 8. (Color online) As in Fig. 7 but for $H_2$. Energies as in Fig. 3. In this case, we have used $R=R_{in}$, where $R_{in}$ is the classical inner turning point of the $v=2$ vibrational level of the residual $H_2^+$ ion.

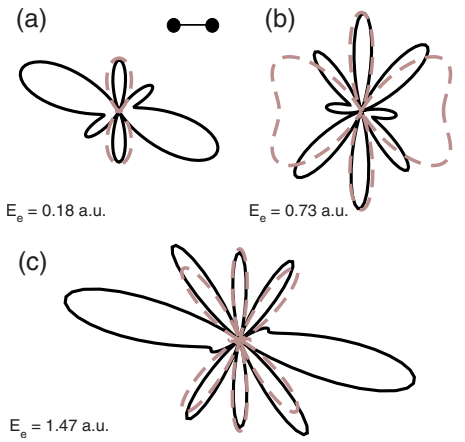


FIG. 9. (Color online) As in Fig. 7 but for $Li_2^+$. Energies as in Fig. 4.

tial $f$-wave contributions, to the continuum wave function that have little to do with diffraction. However, as the energy is raised, the evolution of the distribution with electron energy, in particular the appearance of additional lobes, is increasingly well described by the diffraction model.

It is interesting to note that the results of the one-electron model shown in Figs. 8 and 9 are in much better agreement with the artificial $H_2^+$ results shown in Figs. 5 and 6 than with the true $H_2$ and $Li_2^+$ results. Thus, the apparent failures of the two-dipole antennas model are mainly due to distortions introduced by electron correlation in the single ionization of $H_2$ and $Li_2^+$. Hence, it is not surprising that in the case of double ionization of $H_2$, where correlation is essential even at extreme energy sharing conditions, the one-electron model exhibits the same or even larger deficiencies. In fact, in $H_2$ double ionization, the model only works reasonably well for electron energies larger than 10 a.u. [18].

## IV. CONCLUSION

We have presented a theoretical study of electron angular distributions that arise in photoionization of $H_2^+$, $H_2$, and $Li_2^+$ with circularly polarized light of a few hundred eV (a few tens of eV for $Li_2^+$). At these photon energies, two-center interference effects due to confinement and double-slit diffraction are expected [14]. The present results show that, for $H_2^+$ and $H_2$, the calculated angular distributions for circularly polarized light are very similar to those resulting from the arithmetic average of the calculated distributions for parallel and perpendicular linearly polarized light. This implies that, at these high energies, coherence between the corresponding $\Sigma_u^+$ and $\Pi_u$ amplitudes is not very important, except for a small rotation of the calculated angular distribution that slightly follows the rotation of the polarization vector. The consequence is that confinement and double-slit effects observed in the case of linear polarization are also observed in the case of circular polarization, although, in the latter case, they may be more difficult to identify when they appear at the same electron energy. Furthermore, at the lower photon energies, the multiple lobes observed in the angular distributions for circularly polarized light (which are absent for linearly polarized light) have little to do with confinement and/or double-slit diffraction.

The physical situation is not very different for $Li_2^+$, although, for this particular molecule, confinement and double-slit effects are expected at much lower photon energies. This is the consequence of the large value of the equilibrium internuclear distance (5.9 a.u.). It is for this reason that the angular distributions of $Li_2^+$ obtained with circularly polarized light are more complex, presenting a large number of lobes and nodes that, in any case, are also present in the distributions with linearly polarized light. We have also found that the angular distributions for $H_2^+$ and $H_2$ approximately follow the formula $\cos^2(\mathbf{k}_e \cdot \mathbf{R}/2)$ [13], except again for a small rotation of the true angular distribution that follows the rotation of the polarization field. In the case of $H_2$, the formula does not account properly for the relative magnitude of the different lobes, except at very high electron energy. This is mainly due to the distortion introduced by the second electron through electron correlation. In the case of $Li_2^+$, the large physical size and asymmetry of the molecular ion core introduces higher partial-wave contributions at lower energies that are not due to simple diffraction. However as the energy is increased so that the asymptotic wavelength of the exiting electron is less than the internuclear distance, the simple diffraction formula gives an increasingly good description of the angular distributions.

## ACKNOWLEDGMENTS

Work partially supported by the Spanish Ministerio de Ciencia e Innovación (Contract No. FIS2007-60064) and the European Science Foundation (COST action CM0702). Work at LBNL performed under the auspices of the U.S. DOE under Contract No. DE-AC02-05CH11231 and supported by the U.S. DOE Office of Basic Energy Sciences, Division of Chemical Sciences. C.W.M. acknowledges support from the National Science Foundation (Grant No. PHY-0604628). Calculations were performed at the Barcelona Supercomputer Center Mare Nostrum (Spain), the Centro de Computación Científica UAM (Spain), and NERSC (Berkeley).

[1] N. Stolterfoht *et al.*, Phys. Rev. Lett. **87**, 023201 (2001).
[2] M. Lein, P. P. Corso, J. P. Marangos, and P. L. Knight, Phys. Rev. A **67**, 023819 (2003).
[3] D. Misra, U. Kadhane, Y. P. Singh, L. C. Tribedi, P. D. Fainstein, and P. Richard, Phys. Rev. Lett. **92**, 153201 (2004).
[4] J. Itatani, J. Levesque, D. Zeidler, H. Niikura, H. Pépin, J. C. Kieffer, P. B. Corkum, and D. M. Villeneuve, Nature (London) **432**, 867 (2004).

[5] S. N. Yurchenko, S. Patchkovskii, I. V. Litvinyuk, P. B. Corkum, and G. L. Yudin, Phys. Rev. Lett. **93**, 223003 (2004).
[6] O. A. Fojón, J. Fernández, A. Palacios, R. D. Rivarola, and F. Martín, J. Phys. B **37**, 3035 (2004).
[7] G. L. Kamta and A. D. Bandrauk, Phys. Rev. A **71**, 053407 (2005).
[8] D. Rolles *et al.*, Nature (London) **437**, 711 (2005).
[9] O. A. Fojón, A. Palacios, J. Fernández, R. D. Rivarola, and F. Martín, Phys. Lett. A **350**, 371 (2006).
[10] X. J. Liu *et al.*, J. Phys. B **39**, 4801 (2006).
[11] D. Misra, A. Kelkar, U. Kadhane, A. Kumar, L. C. Tribedi, and P. D. Fainstein, Phys. Rev. A **74**, 060701(R) (2006).
[12] D. Toffoli and P. Decleva, J. Phys. B **39**, 2681 (2006).
[13] D. Akoury *et al.*, Science **318**, 949 (2007).
[14] J. Fernández, O. Fojón, A. Palacios, and F. Martín, Phys. Rev. Lett. **98**, 043005 (2007).
[15] M. Meckel *et al.*, Science **320**, 1478 (2008).
[16] B. Zimmermann *et al.*, Nat. Phys. **4**, 649 (2008).
[17] F. L. Yip, C. W. McCurdy, and T. N. Rescigno, Phys. Rev. A **78**, 023405 (2008).
[18] D. A. Horner, S. Miyabe, T. N. Rescigno, C. W. McCurdy, F. Morales, and F. Martín, Phys. Rev. Lett. **101**, 183002 (2008).
[19] H. D. Cohen and U. Fano, Phys. Rev. **150**, 30 (1966).
[20] I. G. Kaplan and A. P. Markin, Sov. Phys. Dokl. **14**, 36 (1969).
[21] J. Fernández, O. Fojón, and F. Martín, Phys. Rev. A **79**, 023420 (2009).
[22] F. Martín, J. Phys. B **32**, R197 (1999).
[23] A. Lafosse, M. Lebech, J. C. Brenot, P. M. Guyon, L. Spielberger, O. Jagutzki, J. C. Houver, and D. Dowek, J. Phys. B **36**, 4683 (2003).
[24] D. Dowek, J. Fernández, M. Lebech, J. C. Houver, and F. Martín, J. Phys.: Conf. Ser. **88**, 012009 (2007).
[25] H. Bachau, E. Cormier, P. Decleva, J. E. Hansen, and F. Martín, Rep. Prog. Phys. **64**, 1815 (2001).
[26] M. Walter and J. Briggs, J. Phys. B **32**, 2487 (1999).
[27] D. Dill, J. Chem. Phys. **65**, 1130 (1976).
[28] W. Vanroose, D. A. Horner, F. Martín, T. N. Rescigno, and C. W. McCurdy, Phys. Rev. A **74**, 052702 (2006).
[29] I. Sánchez and F. Martín, Phys. Rev. Lett. **79**, 1654 (1997).
[30] I. Sánchez and F. Martín, Phys. Rev. Lett. **82**, 3775 (1999).
[31] F. Martín *et al.*, Science **315**, 629 (2007).
[32] G. Laurent *et al.*, Phys. Rev. Lett. **96**, 173201 (2006).
[33] W. Kołos, K. Szalewicz, and H. J. Monkhorst, J. Chem. Phys. **84**, 3278 (1986).
[34] T. N. Rescigno, D. A. Horner, F. L. Yip, and C. W. McCurdy, Phys. Rev. A **72**, 052709 (2005).
[35] R. Della Picca, P. D. Fainstein, M. L. Martiarena, and A. Dubois, Phys. Rev. A **77**, 022702 (2008).